rine-18-fluorodeoxyuridine, L-[methyl-^{14}C]methionine, [6-^{3}H]thymidine and gallium-67. *J Nucl Med* 1991;32:2118–2123.
17. Rege SD, Chaiken L, Hoh CK, et al. Change induced by radiation therapy in FDG uptake in normal and malignant structures of the head and neck: quantitation with PET. *Radiology* 1993;189:807–812.
18. Lowe VJ, Herbert ME, Hawk TC, Ansher MS, Coleman RE. Chest wall FDG accumulation in serial FDG-PET images in patients being treated for bronchogenic carcinoma with radiation [Abstract]. *J Nucl Med* 1994;35:76P.
19. Kubota K, Matsuzawa T, Takahasi T, et al. Rapid and sensitive response of carbon-11-L-methionine tumor uptake to irradiation. *J Nucl Med* 1989;30:2012–2016.
20. Kubota K, Kubota R, Matsuzawa T. Dose-responsive growth inhibition by glucocorticoid and its receptors in mouse teratocarcinoma OTT6050 in vivo. *Cancer Res* 1983;43:787–793.
21. Kubota K, Ishiwata K, Yamada S, et al. Dose-responsive effect of radiotherapy on the tumor uptake of L-[methyl-^{11}C]methionine; feasibility for monitoring recurrence of tumor. *Nucl Med Biol* 1991;19:27–32.
22. Hall EJ. Time, dose and fractionation in radiotherapy. In: Hall EJ, ed. *Radiobiology for the radiologist*, 4th ed. Philadelphia, PA: Lippincott; 1994:211–229.
23. Lovett EJ, Alderman J, Munster E, Lundy J. Suppressive effects of thiopental and halothane on specific arms of the immune response. *J Surg Oncol* 1980;15:327–334.
24. Steen RG, Wilson DA, Bowser C, Wehrle JP, Glickson JD, Rajan SS. ^{31}P NMR spectroscopic and near infrared spectrophotometric studies of effects of anesthetics on in vivo RIF-1 tumors. *NMR Biomed* 1989;2:87–92.
25. Kimler BF, Liu C, Evans RG, Morantz RA. Effect of pentobarbital on normal brain protection and on the response of 9L rat brain tumor to radiation therapy. *J Neurosurg* 1993;79:577–583.
26. Patz EF, Lowe VJ, Hoffman JM, Paine SS, Harris LK, Goodman PC. Persistent or recurrent bronchogenic carcinoma: detection with PET and 2-[F-18]-2-deoxy-D-glucose. *Radiology* 1994;191:379–382.
27. Kairento AL, Brownell GL, Elmaleh DR, Swartz MR. Comparative measurement of regional blood flow, oxygen and glucose utilization in soft tissue tumor of rabbit with positron imaging. *Br J Radiology* 1985;58:637–643.
28. Cartee GD, Donan AG, Ramlal T, Klip A, Holloszy JO. Stimulation of glucose transport in skeletal muscle by hypoxia. *J Appl Physiol* 1991;70:1593–1600.
29. Bashan N, Burdett E, Hundel HS, Klip A. Regulation of glucose transportand GLUT 1 glucose transporter expression by 3% O2 in muscle cells in culture. *Am J Physiol* 1992;262:682–690.
30. Shetty M, Loeb JN, Ismail-Beigi F. Enhancement of glucose transport in response to inhibition of oxidative metabolism: pre- and posttranslational mechanisms. *Am J Physiol* 1992;262:527–532.
31. Bashan N, Burdett E, Guma A, Sargeant R, Tumiati L, Liu Z, Klip A. Mechanisms of adaptation of glucose transporters to changes in the oxidative chain of muscle and fat cells. *Am J Physiol* 1993;264:430–440.
32. Guerrieri F, Capozza G, Fratello A, Zanotti F, Papa S. Functional and molecular changes in F_0F_1 ATP-synthase of cardiac muscle during aging. *Cardioscience* 1993;4:93–98.
33. Lakatta EG, Yin FC. Myocardial aging: functional alterations and related cellular mechanisms. *Am J Physiol* 1982;242:H927–H941.
34. Kubota K, Kubota R, Yamada S. FDG accumulation in tumor tissue. *J Nucl Med* 1993;34:419–421.
35. Bustos R, Sobrino F. Stimulation of glycolysis as an activation signal in rat peritoneal macrophages. *Biochem J* 1992;282:299–303.
36. Kubota R, Kubota K, Yamada S, Tada M, Ido T, Tamahashi N. Active and passive mechanisms of [fluorine-18] fluorodeoxyglucose uptake by proliferating and prenecrotic cancer cells in vivo: a microautoradiographic study. *J Nucl Med* 1994;35:1067–1075.

Monitoring Gene Therapy with Herpes Simplex Virus Thymidine Kinase in Hepatoma Cells: Uptake of Specific Substrates

Uwe Haberkorn, Annette Altmann, Iris Morr, Karl-Werner Knopf, Christine Germann, Roland Haeckel, Franz Oberdorfer and Gerhard van Kaick

Department of Oncological Diagnostics and Therapy, German Cancer Research Center, Heidelberg, FRG

This study investigates the application of PET with specific substrates for the assesment of enzyme activity after transfer of the herpes simplex virus thymidine kinase (HSV-tk) gene. **Methods:** After transfection of a rat hepatoma cell line with a retroviral vector containing the HSV-tk gene, different clones were established by G418 selection. Uptake measurements were performed up to 48 hr in a TK-expressing cell line and in a control cell line using thymidine (TdR; measured under therapy conditions), fluorodeoxycytidine (FdCyt) and ganciclovir (GCV). Additionally, bystander experiments and inhibition/competition studies were done. **Results:** In TK-expressing cells GCV treatment caused an increased (up to 250%) TdR uptake in the acid-soluble fraction and a decrease to 5.5% in the acid-insoluble fraction. The FdCyt uptake was higher in the TK-expressing cells than in controls with a maximum after 4 hr (12-fold and 3-fold higher in the acid-insoluble and acid-soluble fraction). GCV accumulated up to 180-fold more in the acid-insoluble and 26-fold more in the acid-soluble fraction. GCV uptake occurred mainly by the nucleoside transport systems. Bystander experiments revealed a relation between growth inhibition or GCV uptake and the amount of TK-expressing cells. GCV uptake and growth inhibition were correlated with r = 0.96. **Conclusion:** Assessment of GCV accumulation may serve as an indicator of the enzyme activity and of therapy outcome. TdR may be useful to measure therapy effects on DNA synthesis, whereas the potential of FdCyt has to be investigated in further studies.

Key Words: gene therapy; HSV thymidine kinase; ganciclovir; PET

J Nucl Med 1997; 38:287–294

Received Feb. 12, 1996; revision accepted Jun. 15, 1996.

For correspondence or reprints contact: Uwe Haberkorn, MD, Dept. of Oncological Diagnostics and Therapy, German Cancer Research Center, Im Neuenheimer Feld 280, FRG-Heidelberg 69120, Germany.

Gene therapy is one of the most promising approaches in cancer therapy directed to selectively target and destroy tumor cells. Using recombinant vector systems, suicide genes may be introduced in the malignant cells. These genes encode enzymes, which convert nontoxic prodrugs into highly toxic metabolites. Since retroviruses preferentially infect dividing cells, recombinant retroviral vectors are useful tools for the transfer of genes in proliferating tissues as malignant tumors. Tissue specificity may be achieved by modifying the virus envelope (*1*) or the introduction of tissue or even tumor specific regulatory sequences (*2,3*).

Gene therapy with herpes simplex virus thymidine kinase (HSV-tk) has been performed in a variety of tumor models in vitro and in vivo (*4–9*). In contrast to human thymidine kinase, HSV-tk is less specific and phosphorylates nucleoside analogs such as acyclovir and ganciclovir (GCV) to their monophosphate metabolites (*10*). These monophosphates are subsequently phosphorylated by cellular kinases to the di- and triphosphates. After integration of the GCV metabolites into DNA, chain termination occurs, followed by cell death.

Although it has been shown that not all tumor cells have to be infected to obtain a sufficient therapeutic response (*6,8,9*), repeated injections of the recombinant retroviruses may be necessary until a therapeutic level of enzyme activity in the tumor is reached. Therefore, planning and individualization of gene therapy with the HSV-tk suicide system necessitates the assessment of suicide gene expression in the tumor to decide if: repeated gene transductions of the tumor are necessary, and to establish a therapeutic window of maximum gene expression

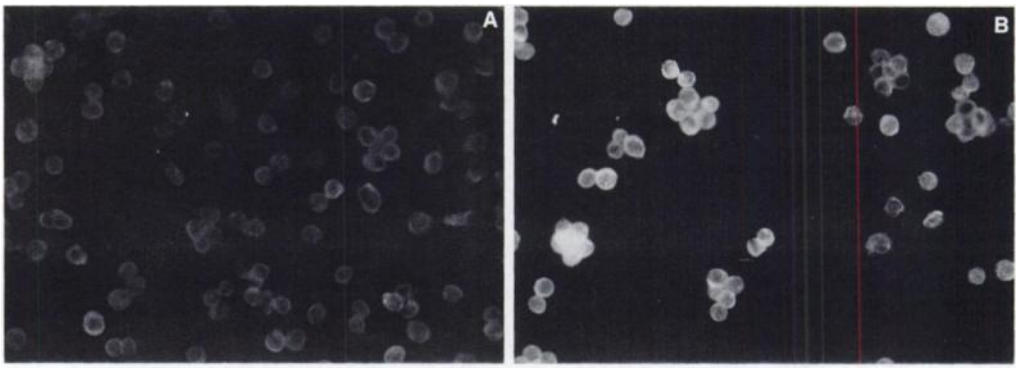

FIGURE 1. Immunostaining of LXSN6 cells (A) and LXSNtk8 cells (B) after incubation with rabbit antiserum against HSV-tk. LXSNtk8 cells show stronger fluorescence in the cytoplasma indicating HSV-tk expression.

and GCV administration. This study was performed to evaluate the application of thymidine and specific substrates of HSV-tk as possible PET tracer for the monitoring of gene therapy with HSV-tk.

MATERIALS AND METHODS

Rat Morris hepatoma cells (MH3924A) were used for all experiments. The cells were maintained in culture flasks in RPMI-1640 medium (Gibco BRL, Eggenstein, FRG) supplemented with 292 mg/liter glutamine, 100,000 IE/liter penicillin, 100 mg/liter streptomycin and 20% fetal calf serum at 37°C, in an atmosphere of 95% air and 5% CO_2.

Cloning and Selection of Cell Lines

For the generation of TK-expressing cell lines, a Pvu II fragment of ptk103 was cloned into the Hpa I site of LXSN (*11*). The correct orientation of the HSV-tk gene in the construct was verified by dideoxynucleotide sequencing. Thereafter, MH3924A cells were transfected with LXSN-tk or with LXSN (= controls) by lipofection (Gibco BRL) and a G418 selection was done. Two cell lines, LXSN6 (control line with the empty vector, in vitro doubling time 17.8 ± 1 hr) and LXSNtk8 (a GCV sensitive line bearing the HSV-tk gene, in vitro doubling time 16.8 ± 0.7 hr) were selected for further studies. Each experiment was done in triplicate at 37°C in an atmosphere of 95% air and 5% CO_2 with cells being in the logarithmic growth phase.

Immunostaining

The cells were trypsinated, washed with culture medium and rotated for 5 min at 1200 rpm in a Heraeus minifuge. The pellet was resuspended in phosphate-buffered saline (PBS) and rotated again for 5 min at 1200 rpm. The resulting pellet was resuspended in PBS (1.6×10^6 cells/ml) and 10 μl were given on microscope slides. The cells were dried at 60°C for 1 hr, fixed for 2 min in −20°C methanol and for 20 min in −20°C acetone and air-dried. Then the cells were incubated in PBS with a polyclonal rabbit anti-TK antibody (dilution 1:25) for 1 hr at 37°C and washed twice for 5 min with PBS. A further incubation step with FITC goat antirabbit IgG antibody (dilution 1:25) was done at 37°C for 1 hr, the cells were washed again twice with PBS and dried. Stronger fluorescence was seen in LXSNtk8 cells than in LXSN6 cells (Fig. 1) indicating expression of TK in LXSNtk8 cells. In the control experiment, with the second antibody alone, no signal was seen.

Thymidine Uptake

The cells were trypsinized, and 1×10^5 cells were seeded in 6-well plates. Two days later, the cells were treated with 0.5 μ*M*, 5 μ*M* and 25 μ*M* GCV. Thymidine (TdR) uptake experiments were performed after 4, 24 and 48 hr incubation in the GCV-containing medium. The cells were pulsed with 185 kBq (methyl-^{3}H) TdR (specific activity 185 GBq/mmole; radioactive concentration 37 MBq/ml; radiochemical purity 97.5%) and cold TdR at a final concentration of 0.05 m*M* for 2 hr in 1 ml medium. After removal of the medium, the cells were washed twice with ice-cold PBS. The lysis was performed with 0.5 *M* perchloric acid (PCA) and a cell scraper. After 30 min on ice, the lysate was vortexed and rotated at 1500 g for 5 min at 0°C. The supernatant was removed, the pellets were washed with 0.5 *M* PCA and rotated again for 5 min at 0°C. The pellet (= acid-insoluble fraction) was resuspended in 1 *M* NaOH at 37°C. The acid-insoluble fraction and the acid-soluble fraction (= both supernatants) were counted using Pico-Fluor-15 (Canberra Packard, Meriden, CT) and a LSC TRICARB 2500TR (Canberra Packard, Meriden, CT) scintillation counter. The measured radioactivity was standardized to the viable cell number as determined by a Coulter counter (Coulter Electronics, Dunstable, Beds., UK) and the trypan blue method (more than 94% viable cells).

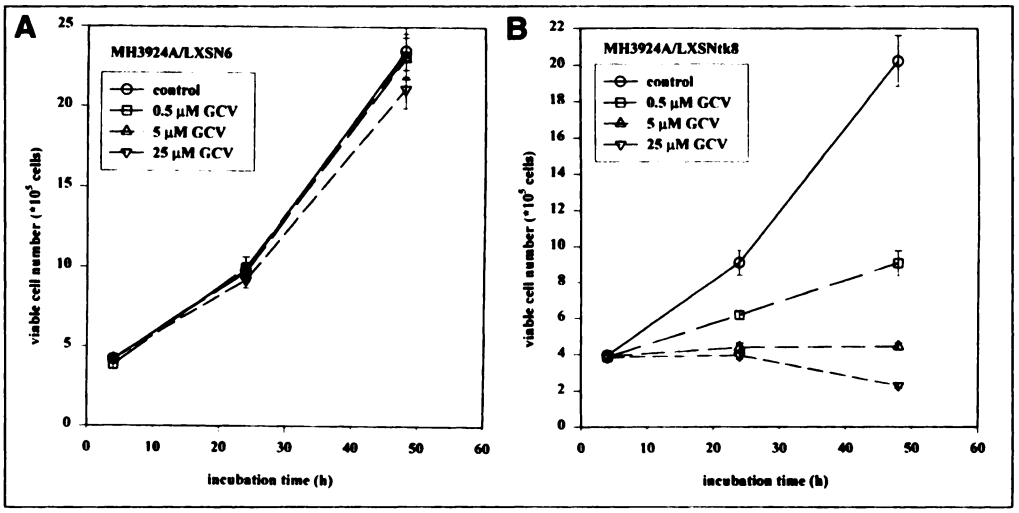

FIGURE 2. Viable cell number of LXSN6 (A) and LXSNtk8 (B) cells. Untreated cells and cells after incubation with 0.5, 5 and 25 μ*M* GCV. Data points represent the mean of 12 measurements.

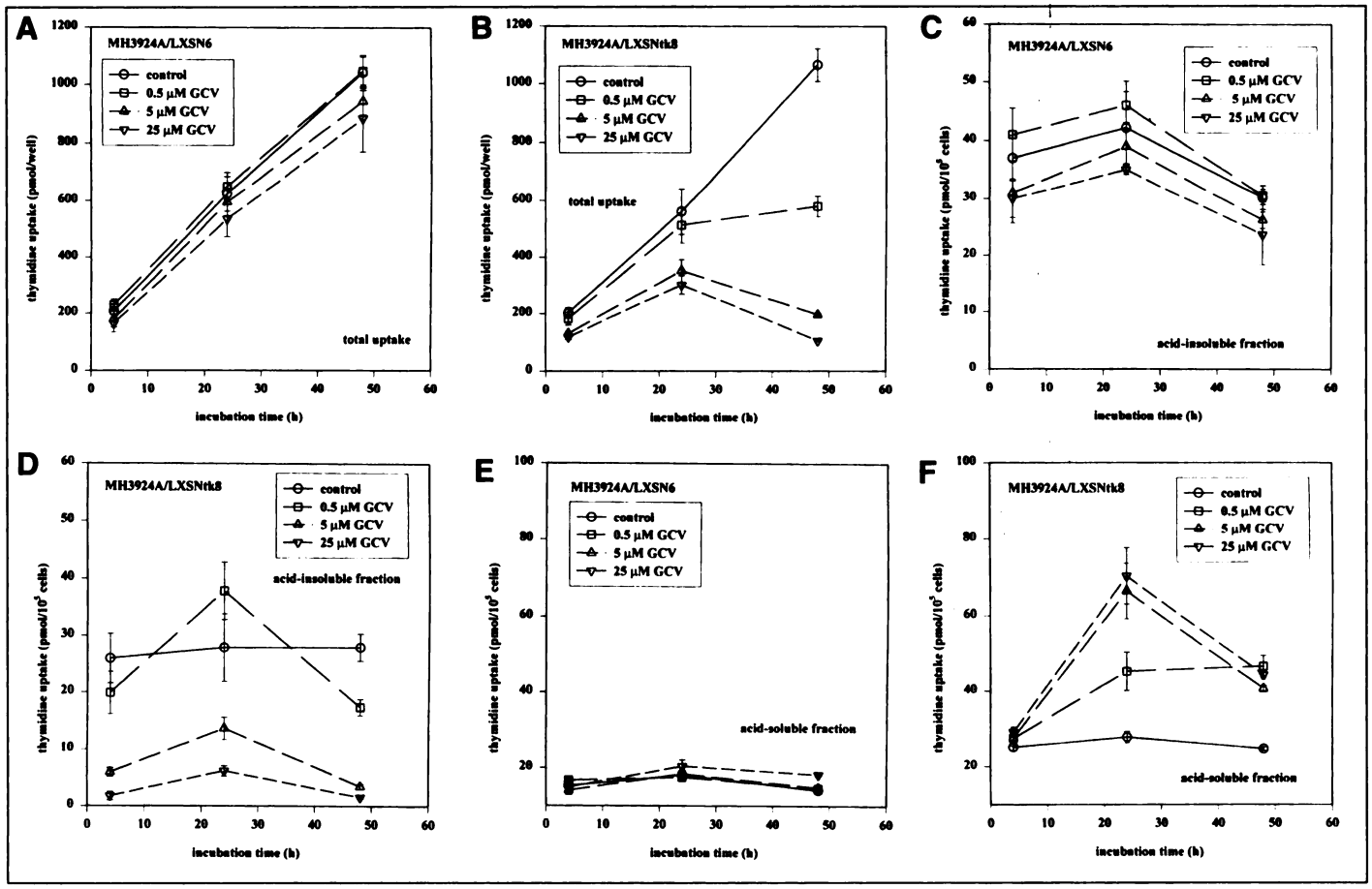

FIGURE 3. Thymidine uptake as pmole/well (A,B) and pmole/10^5 cells (C-F) in LXSN6 and LXSNtk8 cells. Mean and s.d. (n = 3).

Fluorodeoxycytine and GCV Uptake

Two days after seeding of 8×10^4 cells, 185 kBq (8-^{3}H)-GCV (specific activity 662.3 GBq/mmole, radioactive concentration 37 MBq/ml, radiochemical purity 99.5%) or 185 kBq 5-Fluoro-2′-(6-^{3}H)deoxycytidine (specific activity 481 GBq/mmole, radioactive concentration 9.25 MBq/ml, radiochemical purity 99.9%) were added to the culture medium. After incubation times of 10 and 30 min, and 1, 2, 4, 24 and 48 hr, the cells were washed twice with icecold PBS and lysed with icecold 0.5 *M* PCA and a cell scraper. The lysate was incubated on ice for 30 min, vortexed and centrifuged at 1500 g for 5 min at room temperature. The pellet was washed again with ice-cold 0.5 *M* PCA, centrifuged at 1500 g for 5 min and resuspended in 0.3 *M* NaOH. Subsequently the radioactivity was counted in both fractions: the acid-insoluble and the acid-soluble fraction. For chromatographic analysis of the 2-, 4-, 24- and 48-hr lysates, a Waters 600 Multisolvent Delivery system with manual injection (U6K injector) was used. HPLC was performed with a Eurospher 80C8 column (Knauer, Berlin, FRG, particle size 5 μ, 250 × 4 mm). Elution occurred with 2 m*M* NaH_2PO_4 buffer (adjusted to a pH of 3.6 with phosphoric acid) at a flow rate of 1 ml/min. Radioactivity was detected with a Canberra A250 flow-through detection system with a liquid scintillation flow cell (flow volume 500 μl). Retention times for FdCyt and GCV were 9.8 min and 11.7 min on the present setup.

Bystander Experiments

Eight × 10^4 cells were seeded in six-well plates as mixtures of LXSN6 and LXSNtk8 cells with varying amounts of LXSNtk8 cells: 100%, 80%, 40%, 20%, 5% and 0% LXSNtk8 cells. Two days later, the cells were incubated for 4, 24 or 48 hr in the presence of 185 kBq ^{3}H-GCV without further addition of cold GCV (= tracer experiment) and with a final concentration of 5 μ*M* GCV (= therapy experiment). The lysis of the cells was done as described.

Inhibition/Competition Experiments

The cells were washed twice and preincubated for 30 min in Earles balanced salt solution. The medium was removed and fresh EBSS with 185 kBq ^{3}H-GCV was added. The cells were lysed after 10 min incubation with 0.3 N NaOH. For inhibition/competition the uptake experiment was performed in the presence of 2.5 μ*M* dipyridamole, 2.5 μ*M* nitrobenzyl-thioinosine (NBMPR), 1 m*M* TdR, 1 m*M* uracil, 1 m*M* uridine, 1 m*M* adenine and 1 m*M*

TABLE 1
Total Thymidine Uptake (Bq/10^5 cells) in LXSN6 Cells and tk8 Cells after 4, 24 and 48-Hour Exposure with the Indicated Doses of GCV

LXSN6 Cells				tk8 cells			
Dose (μ*M*)	4 hr	24 hr	48 hr	Dose (μ*M*)	4 hr	24 hr	48 hr
0	52.2 ± 4.1	60.0 ± 0.2	44.3 ± 2.6	0	51.1 ± 4.6	55.7 ± 5.1	52.6 ± 2.8
0.5	59.2 ± 5.1	63.7 ± 4.8	45.1 ± 2.2	0.5	47.3 ± 5.7	83.1 ± 10.1	63.9 ± 4.1
5	44.9 ± 6.5	60.2 ± 5.1	41.0 ± 2.1	5	33.5 ± 1.4	80.1 ± 9.2	439 ± 0.9
25	42.6 ± 4.8	58.4 ± 6.6	41.9 ± 5.4	25	30.9 ± 2.0	76.4 ± 8.2	45.8 ± 1.1

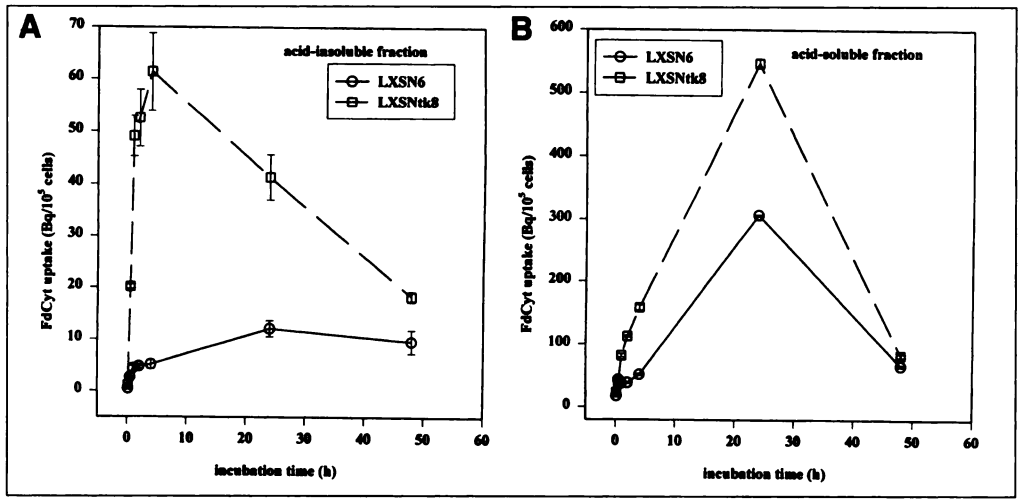

FIGURE 4. Acid-insoluble (A) and acid-soluble (B) fraction of fluorodeoxycytidine uptake (Bq/10^5 cells) in LXSN6 and LXSNtk8 cells after the indicated incubation times. Mean and s.d. (n = 3).

2-chloroadenosine (all Sigma) (*12*). The same was performed with 185 kBq methyl-^{3}H-TdR using 1 m*M* GCV as competitor instead of TdR.

RESULTS

Growth Inhibition and Thymidine Uptake After Treatment with GCV

A dose- and time-dependent growth inhibition was seen in TK-expressing cells after exposure to GCV, with no significant effect in the control cell line (Fig. 2). The TdR uptake/well showed no change in controls and a dose- and time-dependent decrease in TK-expressing cells (Fig. 3A,B). However, standardization to the viable cell number revealed either an increase in treated cells (after 24 hr) or no significant change in the total uptake (Table 1). The radioactivity in the acid-insoluble fraction (representing nucleic acids and proteins) was unchanged in the control cell line (Fig. 3C) and decreased in TK-expressing cells after exposure with 5 and 25 μM GCV to 12% and 5.5% of the untreated cells (Fig. 3D). The acid-soluble fraction (representing unbound radioactivity in the cytoplasma) increased up to 250% of the untreated TK-expressing cells (Fig. 3F) with no change in the control cell line (Fig. 3E).

Uptake of FdCyt and GCV

The FdCyt uptake after 4 hr was 12 times (acid-insoluble fraction) and 3–4 times (acid-soluble fraction) higher in TK-expressing cells than in controls. Since most of the radioactivity (90%) was found in the acid-soluble fraction, the total uptake also showed a 3–4-fold difference. After longer incubation periods the difference in FdCyt uptake between TK-expressing cells and the control cells decreased (1.5–2-fold). The HPLC analysis showed a rapid and almost complete metabolization and degradation in both cell lines. A time dependent increase of GCV uptake could be observed in the acid-insoluble (Fig. 5A) as well as in the acid-soluble (Fig. 5B) fraction of TK-expressing cells, whereas the control cell line rapidly reached a plateau. TK-expressing cells accumulated up to 190-fold (25-fold after 4 hr) more GCV in the acid-insoluble fraction and up to 26-fold (8-fold after 4 hr) more in the acid-soluble fraction. Most of the radioactivity (80%) was found in the acid-soluble fraction resulting in a 30-fold (8-fold after 4 hr) higher total uptake of GCV. The HPLC analysis of this fraction showed unmetabolized GCV in control cells and a time dependent shift of GCV to its phosphorylated metabolite in TK-expressing cells: 3.6 ± 0.9%, 14.3 ± 10%, 42.4 ± 1.9% and 90.5 ± 0.8% were phosphorylated after 2, 4, 24 and 48 hr, respectively. Other peaks than GCV or its metabolite were not visible.

Bystander Experiments

The GCV uptake was related to the percentage of TK-expressing cells for all incubation times in the tracer experiment (Fig. 6A,C,E; Table 2) and in the therapy experiment (Fig. 6B,D,F; Table 2). Compared to the controls (100% LXSN6 cells) the mixtures containing TK-expressing cells showed a 3-fold (5% TK-expressing cells, 4 hr incubation) up to a 138-fold (100% TK-expressing cells, 48 hr incubation) higher uptake. Five percent TK-expressing cells caused a 20% and 30% growth inhibition, whereas 100% TK-expressing cells

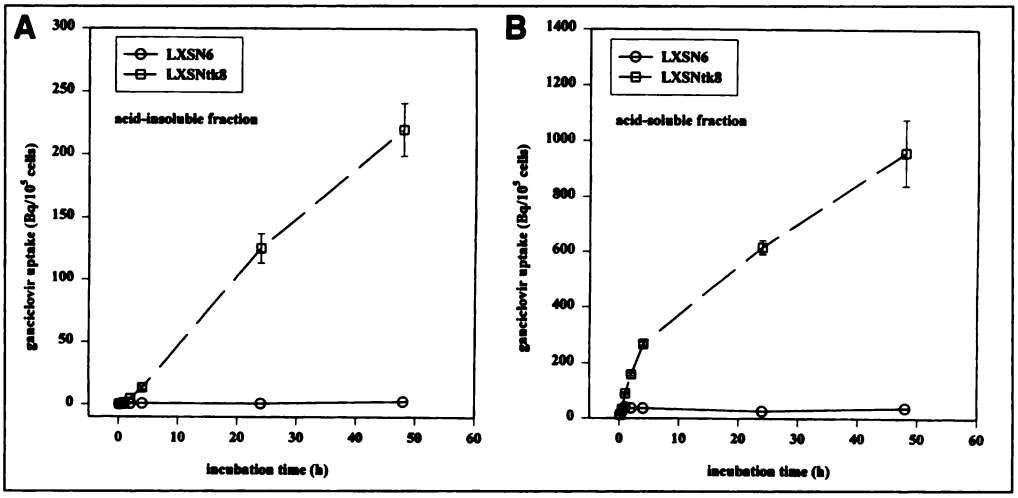

FIGURE 5. Acid-insoluble (A) and acid-soluble (B) fraction of GCV uptake (Bq/10^5 cells) in LXSN6 and LXSNtk8 cells after the indicated incubation times. Mean and s.d. (n = 3).

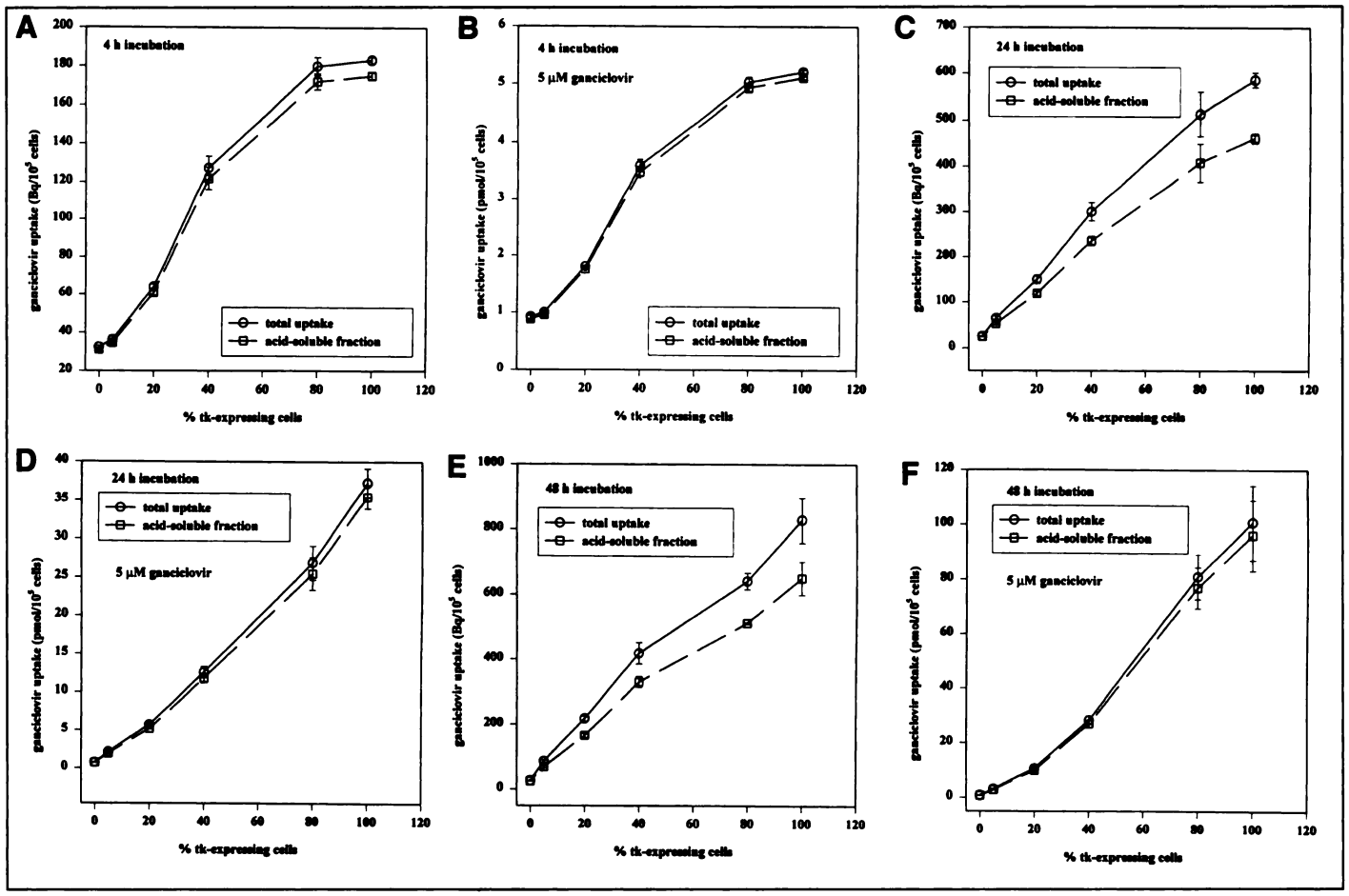

FIGURE 6. GCV uptake in different mixtures of control cells and TK-expressing cells after 4 (A,B), 24 (C,D) and 48 hr (E,F) incubation either with tracer amounts of GCV (A,C,E) or with a final concentration of 5 μM GCV (B,D,F).

resulted in a 60% and 80% inhibition, after 24 hr and 48 hr incubation respectively (Fig. 7A). The total GCV uptake after 24 hr and 48 hr incubation in the tracer experiment was correlated to the growth inhibition after 24 hr and 48 hr exposure to 5 μM GCV with r = 0.94 [Fig. 7B; significant at the 0.1% level (*13*)]. The uptake in the therapy experiment and the growth inhibition were also correlated (r = 0.93). To assess whether the 4 hr uptake value can be used as a predictor of therapy outcome this value was compared to the growth inhibition obtained with the same cultures after 24 hr and 48 hr treatment with high correlations (Fig. 7C; r = 0.96 and r = 0.93).

Inhibition/Competition Experiments

TK-expressing cells accumulated more GCV than the control cells (Fig. 8). No effect of uracil on the GCV uptake was seen in both cell lines, whereas adenine caused a 30% decrease (Fig. 8A, B). After incubation with dipyridamole and NBMPR a 40% and 60% decrease in tracer uptake was observed. TdR, uridine and chloroadenosine caused a higher inhibition with a maximum of 70% to 80% for chloroadenosine (Fig. 8A, B). TdR uptake showed a similar pattern of inhibition and competition: the uptake was also higher in the TK-expressing cell line and no inhibition of tracer accumulation was seen after competition with uracil (Fig. 8C + D). A 20% inhibition was seen with adenine. Dipyridamole and chloroadenosine caused a strong decrease of 93% and 97%, respectively (Fig. 8C, D). The differences in the GCV as well as in the TdR experiment were all significantly different with $p < 0.001$ except for adenine and uracil.

TABLE 2A
Radioactivity in Acid-Insoluble Fraction (Bq/10^5 Cells) after 4-, 24- and 48-Hour Incubation of Different Mixtures of LXSN6 and tk8 Cells*

%tk8 cells	4 hr	24 hr	48 hr
100	8.17 ± 0.1	124.6 ± 6.9	178.7 ± 2.2
80	7.9 ± 0.6	105.1 ± 7.5	129.7 ± 27.8
40	5.5 ± 0.3	64.6 ± 10.1	89.5 ± 16.3
20	3.0 ± 0.1	31.2 ± 4.2	52.9 ± 3.1
5	1.7 ± 0.1	11.7 ± 2.8	18.2 ± 1.1
0	1.3 ± 0.07	1.2 ± 0.4	0.9 ± 0.07

*GCV was added in tracer amounts.

TABLE 2B
Radioactivity in Acid-Insoluble Fraction (fmole/10^5 Cells) after 4-, 24- and 48-Hour Incubation of Different Mixtures of LXSN6 and tk8 Cells*

%tk8 cells	4 hr	24 hr	48 hr
100	94.8 ± 3.6	1819.8 ± 180.2	4642.3 ± 536.8
80	94.5 ± 1.8	1417.3 ± 163.3	4053.3 ± 400.2
40	75.0 ± 5.3	781.2 ± 65.4	1395.9 ± 90.1
20	52.4 ± 2.3	565.1 ± 91.4	753.6 ± 101.9
5	38.2 ± 3.1	151.8 ± 10.4	194.5 ± 14.1
0	40.0 ± 2.1	34.8 ± 4.6	27.8 ± 6.9

*Cold GCV was added to a final concentration of 5 μM.

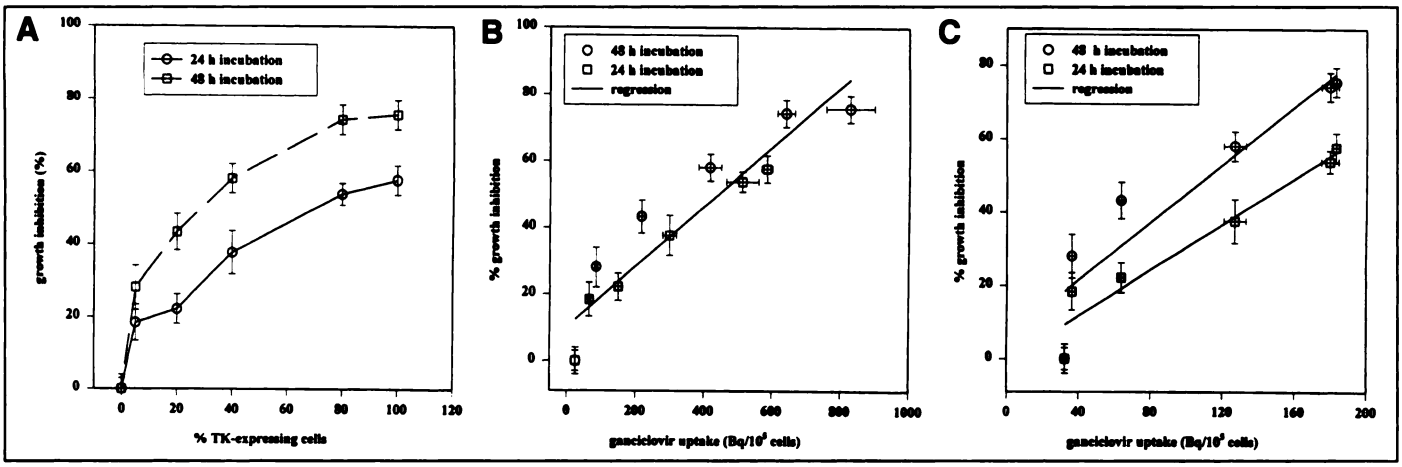

FIGURE 7. Growth behavior of different mixtures of control cells and TK-expressing cells after 24 and 48 hr incubation with 5 μM GCV (A). Relation of total GCV uptake in the tracer experiment (24 and 48 hr incubation) and the growth inhibition after 24 and 48 hr exposure to 5 μM GCV (B). Relation of total GCV uptake in the tracer experiment (4 hr incubation) and the growth inhibition after 24 and 48 hr exposure to 5 μM GCV (C).

DISCUSSION

Morris hepatoma cells transfected with a retroviral vector bearing the HSV-tk gene show expression of the protein (Fig. 1), a dose-dependent growth inhibition after incubation with GCV (Fig. 2) and a dose-dependent decrease of the total TdR uptake/well (Fig. 3), indicating a possible influence of the viable cell number in the clinical situation. Normalization to the viable cell number showed either an increase in treated cells (after 24 hr) or no significant difference in total uptake between treated cells and control cells (Table 1). However, an evaluation of the different fractions revealed a decrease in the nucleic acid fraction and an increase in the acid-soluble fraction (Fig. 3).

The decrease of radioactivity in the nucleic acid fraction occurs early (4 hr) after exposure of the cells to GCV and represents DNA chain termination induced by the HSV-tk-GCV system. The phenomenon of a post-therapeutic increase of TdR or its metabolites in the acid-soluble fraction was observed in former studies after chemo- or radiotherapy (*14,15*). This effect may be explained by an increase in the activity of salvage pathway enzymes (e.g., of host thymidine kinase activity during repair of cell damage). Therefore, it is unlikely that a quantitation with a standardized uptake value is usefull for the determination of the proliferation in treated tumors. The correct interpretation of the PET signal (representing the total radioactivity in a given tissue volume) needs information about TdR metabolism and the size of the different metabolite fractions in

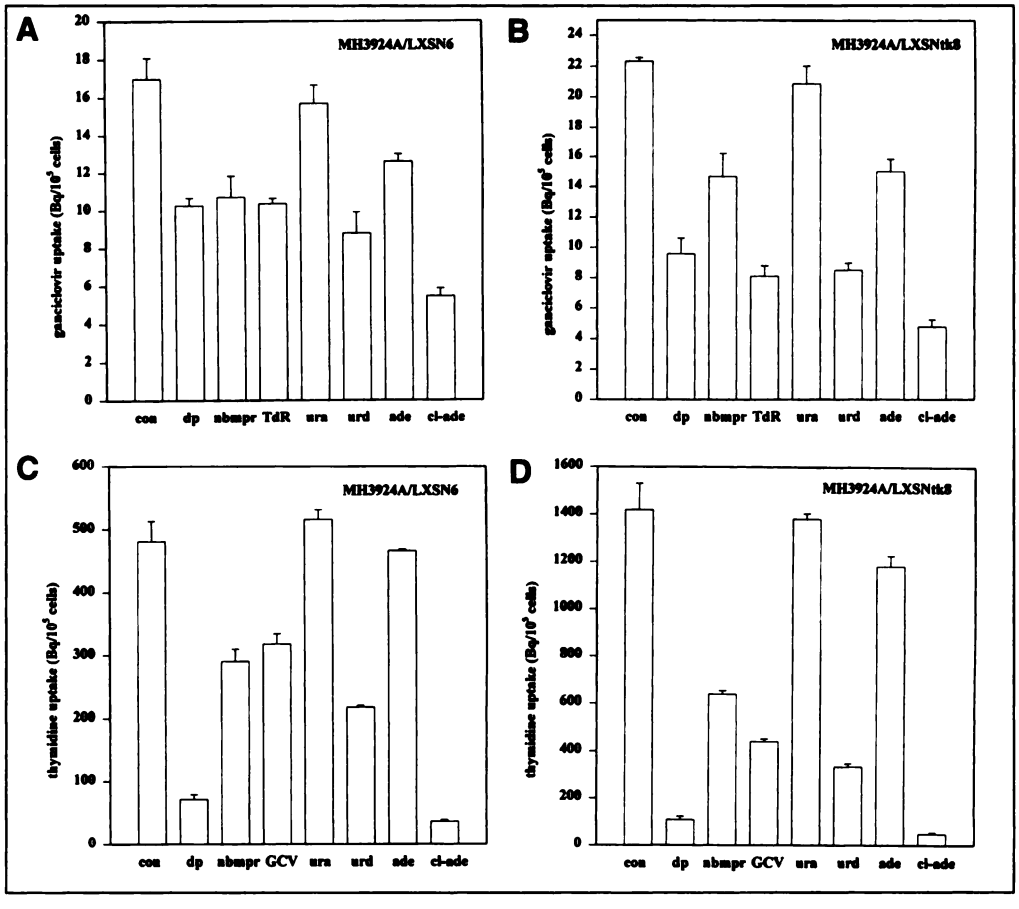

FIGURE 8. GCV (A,B) and thymidine (C,D) uptake in LXSN6 and LXSNtk8 cells after 10 min incubation without and in the presence of dipyridamole (dp), nitrobenzyl-thioinosine (nbmpr), thymidine (TdR) or ganciclovir (GCV), uracil (ura), uridine (urd), adenine (ade) and 2-chloroadenosine (cl-ade). Mean and s.d. (n = 3).

the tumor (*16,17*). Therefore, PET measurements with ^{11}C-TdR may be used to assess the effects of the HSV-tk-GCV system on DNA synthesis if quantitation is based on a modeling approach.

FdCyt and other halogenated analogs of deoxycytidine have been reported as specific substrates for HSV-tk (*18,19*). In our study, the FdCyt uptake was higher in TK-expressing than in control cells with a maximum after 4–6 hr (Fig. 4). After longer incubation periods the FdCyt uptake declined. HPLC analysis showed a rapid and almost complete metabolization and degradation in both cell lines, which might be due to dehalogenation or the action of nucleosidases. The GCV uptake showed a time-dependent increase in TK-expressing cells and a plateau in control cells (Fig. 5). The HPLC analysis revealed unmetabolized GCV in control cells and a time dependent shift of GCV to its phosphorylated metabolite in TK-expressing cells The difference in total GCV uptake between TK-expressing cells and control cells was higher (8-fold after 4 hr, 30-fold after 48 hr) than for FdCyt (3–4-fold after 4 hr, 1.5–2-fold after 48 hr). GCV can be labeled with ^{18}F and therefore is a candidate for PET measurements (*20*). Due to the higher difference in tracer uptake and the high degradation of FdCyt, the use of labeled GCV for quantitative PET studies seems to be superior to labeled FdCyt. In a recent study, 5-iodo-2′-fluoro-2′deoxy-1-β-D-arabinofuranosyluracil (FIAU) was reported as a better marker substrate for TK activity (*21*). However, the authors related the FIAU uptake to the GCV sensitivity and the level of TK expression in bulk cultures of transduced cell lines or in different cell lines. Therefore, differences of the integration site and possible inactivation of the viral promoter may influence the FIAU uptake in this study. In our study differences in TK expression were simulated by the mixture of a single stably transfected cell line (LXSNtk8) with a control cell line (LXSN6).

Not every tumor cell needs to express HSV-tk to result in complete tumor regression (*6,8,9*). Tumor cells in close proximity of TK-expressing cells become sensitive to GCV, a phenomenon, which has been called "bystander effect." Two explanations have been proposed: transfer of phosphorylated GCV via gap junctions (*22*) or uptake of the phosphorylated metabolite via apoptotic vesicles (*23*). In rat glioma cells, Chen et al. (*24*) showed that above a certain enzyme level threshold this bystander effect depends on the levels of the HSV-tk expression. Therefore, measurements of the enzyme activity are important for the management of gene therapy with HSV-tk. Since the enzyme phosphorylates GCV to the negatively charged GCV-monophosphate, which cannot penetrate the plasma membrane, a trapping of this metabolite occurs. Therefore, the amount of trapped radiolabeled GCV reflects the enzyme activity. Furthermore the total accumulation of labeled GCV in the whole tumor, i.e., in TK-expressing cells as well as in cells which lack TK-expression, but are in close proximity of TK-expressing cells, may be an indicator of the bystander effect. To assess, whether the measurement of GCV uptake can be used to estimate the enzyme activity as well as the possible bystander effect, experiments were performed with mixtures of varying amounts of TK-expressing and control cells. In these experiments we found a dependence of the growth inhibition and the GCV uptake on the percentage of TK-expressing cells (Figs. 6 and Fig. 7) with the growth inhibition being highly correlated to the GCV uptake with $r = 0.94$. Due to the half life of ^{18}F shorter incubation times than 24 or 48 hr have to be evaluated for a correct simulation of the PET study. Therefore, the 4 hr uptake value was compared to the growth inhibition after 24 hr and 48 hr treatment with high correlations ($r = 0.96$ and $r = 0.93$). This indicates, that the amount of GCV accumulation even after short exposure times can be used as a predictor of therapy outcome. PET studies with tracer amounts of labeled GCV may be used to estimate the level of HSV thymidine kinase activity in the tumor. However, only a small part of the tumor will be infected in vivo and also instability of gene expression may occur, especially with retroviral promoters. Therefore, it is not clear yet whether the PET signal will be strong enough to result in a clear cut distinction between therapy responders and nonresponders.

Two classes of nucleoside transporters have been described: the equilibrative, facilitated diffusion systems and the concentrative, sodium-dependent systems (*25–27*). In our experiments competition for all concentrative nucleoside transport systems and inhibition of the GCV transport by the equilibrative transport systems (Fig. 8) was observed, whereas the nucleobase systems showed no significant contribution to the GCV uptake. In human erythrocytes acyclovir has been shown to be transported mainly by the purine nucleobase carrier (*28*). Due to a hydroxymethyl group on its side chain, GCV has a stronger similarity to nucleosides and, therefore, may be transported also by a nucleoside transporter (*29*). Experiments in human erythrocytes revealed that GCV permeates the membrane by the purine nucleobase carrier and by nucleoside transport (*30,31*). In our experiments GCV was mainly transported by the nucleoside transport systems. We also observed that the TdR uptake was higher in TK-expressing cells than in controls. Since TdR is a substrate for HSV-tk, the modified cells have an enhanced phosphorylating capacity, which may explain this phenomenon.

CONCLUSION

TdR may be used to measure the effects of the HSV-tk suicide system on DNA synthesis and the assessment of GCV accumulation may serve as an indicator of the enzyme activity and, therefore, of therapy outcome. Since GCV is transported by the nucleoside carriers and trapped after phosphorylation, this suicide system seems to be superior for therapy monitoring than 5-fluorocytosine and cytosine deaminase, because 5-fluorocytosine enters the cell by passive diffusion and also shows rapid efflux (*32*). However, animal experiments are needed to assess whether the in vivo signal obtained with PET is sufficient to obtain significant differences for a cutoff between therapy responders and nonresponders.

ACKNOWLEDGEMENTS

We thank P.S. Conti and A. Shields for fruitful discussions, A. Runz for excellent technical assistance and M. Pawhita for supplying the ptk103.

REFERENCES

1. Kasahara N, Dozy AM, Kan YW. Tissue-specific targeting of retroviral vectors through ligand-receptor interactions. *Science* 1994;266:1373–1376.
2. Huber BE, Richards CA, Krenitsky TA. Retroviral-mediated gene therapy for the treatment of hepatocellular carcinoma: an innovative approach for cancer therapy. *Proc Natl Acad Sci USA* 1991;88:8039–8043.
3. Vile RG, Hart IR. Use of tissue-specific expression of the herpes simplex virus thymidine kinase gene to inhibit growth of established murine melanomas following direct intratumoral injection of DNA. *Cancer Res* 1993;53:3860–3864.
4. Chen SH, Shine HD, Goodman JC, Grossman RG, Woo SLC. Gene therapy for brain tumors: regression of experimental gliomas by adenovirus-mediated gene transfer in vivo. *Proc Natl Acad Sci USA* 1994;91:3054–3057.
5. Moolten FL. Tumor chemosensitivity conferred by inserted herpes thymidine kinase genes: paradigm for a prospective cancer control strategy. *Cancer Res* 1986;46:5276–5281.
6. Caruso M, Panis Y, Gagandeep S, Houssin D, Salzmann JL, Klatzman D. Regression of established macroscopic liver metastases after in situ transduction of a suicide gene. *Proc Natl Acad Sci USA* 1993;90:7024–7028.
7. Oldfield EH, Ram Z, Culver KW, Blaese RM, DeVroom HL, Anderson WF. Gene therapy for the treatment of brain tumors using intra-tumoral transduction with the thymidine kinase gene and intravenous ganciclovir. *Hum Gene Ther* 19931:39–69.
8. Culver KW, Ram Z, Walbridge S, et al. In vivo gene transfer with retroviral vector-producer cells for treatment of experimental brain tumors. *Science* 1992;256:1550–1552.

9. Ram Z, Culver WK, Walbridge S, et al. In situ retroviral-mediated gene transfer for the treatment of brain tumors in rats. *Cancer Res* 1993;53:83–88.
10. Keller PM, Fyfe JA, Beauchamp L, et al. Enzymatic phosphorylation of acyclic nucleoside analogs and correlations with antiherpetic activities. *Biochem Pharmacol* 1981;30:3071–3077.
11. Miller AD, Rosman GJ. Improved retroviral vectors for gene transfer and expression. *Bio Techniques* 1989;7:980–990.
12. Zimmerman TP, Mahony WB, Prus KL. 3'-azido-3'deoxythymidine. An unusual nucleoside analogue that permeates the membrane of human erythrocytes and lymphocytes by nonfacilitated diffusion. *J Biol Chem* 1987;262:5748–5754.
13. Sachs L. *Angewandte Statistik*. Berlin. Springer; 1984:329–333.
14. Haberkorn U, Oberdorfer F, Klenner T, et al. Metabolic and transcriptional changes in osteosarcoma cells treated with chemotherapeutic drugs. *Nucl Med Biol* 1994;21:835–845.
15. Higashi K, Clavo AC, Wahl RL. In vitro assessment of 2-fluoro-2-deoxy-D-glucose, L-methionine and thymidine as agents to monitor the early response of a human adenocarcinoma cell line to radiotherapy. *J Nucl Med* 1993;34:773–779.
16. Shields AF, Coonrod DV, Quackenbush RC, Crowley JJ. Cellular sources of thymidine nucleotides: studies for PET. *J Nucl Med* 1987;28:1435–1440.
17. Shields AF, Lim K, Grierson J, Link J, Krohn KA. Utilization of labeled thymidine in DNA synthesis: studies for PET. *J Nucl Med* 1990;1990:31:337–342.
18. Balzarini J, Bohman C, Walker RT, DeClerqu E. Comparative cytostatic activity of different antiherpetic drugs against herpes simplex virus thymidine kinase gene-transfected tumor cells. *Mol Pharmacol* 1994;45:1253–1258.
19. Wohlrab F, Jamieson AT, Hay J, Mengel R, Guschlbauer W. The effect of 2'-fluoro-2'-deoxycytidine on herpes virus growth. *Biochim Biophys Acta* 1985;824: 233–242.
20. Monclus M, Luxen A, Van Naemen J, et al. Development of PET radiopharmaceuticals for gene therapy: synthesis of 9-((1-(^{18}F)fluoro-3-hydroxy-2-propoxy)methyl) guanine. *J Label Comp Radiopharm* 1995;37:193–195.
21. Tjuvajev JG, Stockhammer G, Desai R, et al. Imaging the expression of transfected genes in vivo. *Cancer Res* 1995;55:6126–6132.
22. Bi WL, Parysk LM, Warnick R, Stambrook PJ. In vitro evidence that metabolic cooperation is responsible for the bystander effect observed with HSV-tk retroviral gene therapy. *Hum Gene Ther* 1993;4:725–731.
23. Freeman SM, Abbond CN, Whartenby KA, et al. The "bystander effect": tumor regression when a fraction of tumor mass is genetically modified. *Cancer Res* 1993;53:5274–5283.
24. Chen CY, Chang YN, Ryan P, Linscott M, McGarrity GJ, Chiang YL. Effect of herpes simplex virus thymidine kinase expression levels on ganciclovir-mediated cytotoxicity and the "bystander effect". *Hum Gene Ther* 1995;6:1467–1476.
25. Plagemann PGW, Richey DP. Transport of nucleosides, nucleic acid bases, choline and glucose by animal cells in culture. *Biochem Biophys Acta* 1974;344:263–305.
26. Belt JA, Marina NM, Phelps DA, Crawford CR. Nucleoside transport in normal and neoplastic cells. *Advan Enzyme Regul* 1993;33:235–252.
27. Huang QQ, Yao SYM, Ritzel MWL, Paterson ARP, Cass CE, Young JD. Cloning and functional expression of a complementary DNA encoding a mammalian nucleoside transport protein. *J Biol Chem* 1994;269:17757–17760.
28. Mahony WB, Domin BA, McConnel RT, Zimmerman TP. Acyclovir transport into human erythrocytes. *J Biol Chem* 1988;263:9285–9291.
29. Gati WP, Misra HK, Knaus EE, Wiebe LI. Structural modifications at the 2' and 3' positions of some pyrimidine nucleosides as determinants of their interaction with the mouse erythrocyte nucleoside transporter. *Biochem Pharmacol* 1984;33:3325–3331.
30. Mahony WB, Domin BA, Zimmerman TP. Ganciclovir permeation of the human erythrocyte membrane. *Biochem Pharmacol* 1991;41:263–271.
31. Domin BA, Mahony WB, Zimmerman TP. Membrane permeation mechanisms of 2',3'-dideoxynucleosides. *Biochem Pharmacol* 1993;46:725–729.
32. Haberkorn U, Oberdorfer F, Gebert J, et al. Monitoring of gene therapy with cytosine deaminase: in vitro studies using ^{3}H-5-fluorocytosine. *J Nucl Med* 1996;37:87–94.

Technetium-99m Labeling and Biodistribution of Anti-TAC Disulfide-Stabilized Fv Fragment

Tae M. Yoo, Hye K. Chang, Chang W. Choi, Keith O. Webber, Nhat Le, In S. Kim, William C. Eckelman, Ira Pastan, Jorge A. Carrasquillo and Chang H. Paik

Department of Nuclear Medicine and Positron Emission Tomography Department, Warren G. Magnuson Clinical Center and Laboratory of Molecular Biology, Division of Cancer Biology, Diagnosis and Centers, National Cancer Institute, National Institutes of Health, Bethesda, Bethesda, Maryland

We used a preformed ^{99m}Tc chelate approach to label a genetically engineered disulfide-bonded Fv fragment of anti-Tac monoclonal antibody (dsFv). The biodistribution of this ^{99m}Tc-labeled dsFv was evaluated in athymic mice with IL-2α-receptor-positive ATAC4 tumor xenografts. **Methods:** Benzoylmercaptoacetyl-triglycine (Bz-MAG3) was first labeled with ^{99m}Tc, and the carboxy group of ^{99m}Tc-MAG3 was then activated to the corresponding tetrafluorophenyl ester. This activated ester was purified with a Sep-Pak C_{18} column and conjugated to dsFv. The resulting ^{99m}Tc-MAG3-dsFv was purified with PD-10 size-exclusion chromatography. The immunoreactivity of ^{99m}Tc-MAG3-dsFv was 76% ± 9%. When incubated in serum at 37°C for 24 hr, there was no appreciable dissociation of ^{99m}Tc. The mice were co-injected with ^{125}I-dsFv labeled by the Iodo-Gen method as a control. The mice were killed at 15 to 720 min for analysis of biodistribution and radiocatabolites. **Results:** The tumor uptake of ^{99m}Tc-MAG3-dsFv was similar to that of ^{125}I-dsFv. The tumor uptake of ^{99m}Tc-MAG3-dsFv was rapid with a tumor-to-blood or tumor-to-organ ratio higher than 1 for all organs except the kidneys. The peak tumor value of 5.1% injected dose per gram was obtained at 45 min, and the tumor-to-organ ratios increased steadily over time; a ratio of 15, 11, 7, 95 and 0.10 resulted at 6 hr for blood, liver, stomach, muscle and kidney. The radioactivity was primarily excreted through kidneys. **Conclusion:** The rapid achievement of high tumor-to-blood and -tissue ratios makes ^{99m}Tc-MAG3-dsFv a promising agent for scintigraphic detection of various hematological malignancies that express IL-2α receptors.

Received Dec. 12, 1995; revision accepted Apr. 5, 1996.

For correspondence or reprints contact: Chang H. Paik, PhD, Department of Nuclear Medicine, Bldg. 21, Rm. 136, Bethesda, MD 20892-1180.

Key Words: technetium-99m; Fv fragment; monoclonal antibody; radioimmunodetection; athymic mice

J Nucl Med 1997; 38:294-300

Anti-Tac dsFv is a genetically engineered antibody fragment that consists of portions of the heavy- and light-chain domains linked by an interchain disulfide bridge and binds to the p55 subunit of the IL-2 receptor (*1,2*). This dsFv is different from single-chain Fv (scFv) in that the heavy- and light-chain domains of scFv are linked by a covalent peptide bond (*3–5*). Because of their small size (~25 kDa), these fragments penetrate tumors much faster (*6–8*) and show more uniform distribution (*9,10*) than intact IgG. In addition, it is expected that the fragments are less immunogenic than IgG, thereby minimizing the development of human antimouse immune response (HAMA) (*11,12*). We have previously reported the biodistribution of anti-Tac dsFv radiolabeled with ^{125}I and ^{18}F in athymic mice bearing antigen-positive tumor xenografts (*13*). The blood clearance, whole-body clearance and tumor targeting occurred quickly, suggesting that ^{99m}Tc-labeled dsFv could be used effectively.

Technetium-99m is the ideal isotope for imaging applications. Both direct and indirect methods for ^{99m}Tc labeling of monoclonal antibody have been reported (*14–20*). Direct labeling approaches require reduction of the disulfide bridge to generate sulfhydryl groups for the formation of a stable complex with ^{99m}Tc unless a sulfhydryl-containing amino acid,